Brazilian Journal of Physics (2018) 48:398–405
https://doi.org/10.1007/s13538-018-0573-9

SOCIEDADE BRASILEIRA DE FÍSICA

ATOMIC PHYSICS

A Theoretical Study on *N′*-[(*Z*)-(4-Methylphenyl)Methylidene] -4-Nitrobenzohydrazide (NMPMN)

Muhammet Okur[1] · Nazmiye Albayrak[2] · Ömer Tamer[3] · Davut Avcı[3] · Yusuf Atalay[3]

Received: 27 November 2017 / Published online: 2 May 2018

Abstract
Quantum mechanical calculations of ground state energy, vibration wavenumbers, and electronic absorption wavelengths of *N′*-[(*Z*)-(4-methylphenyl)methylidene]-4-nitrobenzohydrazide with C15H13N3O3 empirical formula was performed by using Gaussian 09 program. Becke's three-parameter exchange functional in conjunction with the Lee-Yang-Parr correlation functional and Heyd-Scuseria-Ernzerhof functional levels of density functional theory (DFT) with the 6-311++G(d,p) basis set were used in the performing of above mentioned calculations. The highest occupied and lowest unoccupied molecular orbital (HOMO and LUMO) energies have been also calculated at the same levels. Stability of the molecule arising from hyperconjugative interactions and charge delocalization has been analyzed using natural bond orbital (NBO) analysis. Nonlinear optical (NLO) behavior of the title molecule has been examined by the determining of electric dipole moment (μ), polarizability (α), and static first-order hyperpolarizability (β). Finally, molecular electrostatic potential (MEP) surface as well as Mulliken and NBO atomic charges were calculated by using Gaussian 09 program.

Keywords FT-IR · Raman · DFT · Nonlinear optic · NMPMN · Nitrobenzohydrazide · NBO

1 Introduction

In recent times, extensive studies have been made on the synthesis and crystal growth of nonlinear optical (NLO) material because of their potential application in the field of telecommunication, optical signal processing and optical switching [1]. Much attention has been given to organic nonlinear optical materials since the nonlinear optical responses in this broad class of materials are microscopic in origin, offering an opportunity to use theoretical modeling coupled with flexibility to design and produce novel materials [1, 2]. Intensive theoretical and experimental investigations on these materials have played a vital role in bringing about understanding the microscopic origin of nonlinear optical behavior of organic materials [3, 4]. For the higher nonlinear optical efficiency, one requires highly polarizable molecular systems having asymmetric charge distribution in the molecule, which are substituted donor and acceptor groups at the ends of the molecule with noncentrosymmetric crystal structure [5].

Nonlinear optical properties of organic materials have been known with their dependence on the polarizability nature of π-bonds. The best way that enhances the delocalized π-electrons in the conjugated system is recognized as the adding donor and acceptor groups. It is well known that the conditions such as the π-conjugated bridge lengths, the number of the aromatic rings, and the substitution of molecular system with electron donor or/and electron acceptor groups can lead to improve the nonlinear optical efficiency [5].

In NMPMN, *N′*-[(*Z*)-(4-methyl phenyl)methylidene]-4-nitrobenzohydrazide [6], the electron donor methyl group (-CH_3) and electron acceptor nitro group (-NO_2) have been coordinated to the opposite ends of the conjugated system. It was previously reported that the penetrations of electron donor and acceptor groups to opposite sides increase the symmetric and asymmetric charge distributions through the molecular system [7]. The delocalization length between the methyl and nitro substituted phenyl rings are remarkable in terms of the high nonlinearity. The C=N, C=O, and N-N bonds have

✉ Nazmiye Albayrak
noneralbayrak@icloud.com

[1] Vocational School of Health Services, Bilecik Seyh Edebali University, 11210 Bilecik, Turkey

[2] Vocational School of Health Services, Biruni University, 34010 Istanbul, Turkey

[3] Faculty of Arts and Sciences, Department of Physics, Sakarya University, 54187, Serdivan, Sakarya, Turkey

been also known to increase the intramolecular charge transfer (ICT) including nonlinear optical activity of investigated systems.

In the last decade, organic nonlinear optical materials structural, spectroscopic, electronic, and nonlinear optical properties have been reported by using theoretical methods [8–10]. Nonetheless, to the best of our knowledge, the theoretical investigations on structural, spectroscopic, electronic, and nonlinear optical properties of NMPMN have not been performed yet. In the present paper, we used DFT theory in order to investigate structural, spectroscopic, and electric properties as well as NLO and natural bond orbital (NBO) analysis for title molecule.

1.1 Computational Details

All of the quantum mechanical calculations were carried out by using density functional theory (DFT) employing Becke's three-parameter exchange functional in conjunction with the Lee-Yang-Parr correlation functional (B3LYP) [11, 12] and the recommended version of the full Heyd-Scuseria-Ernzerhof functional (HSEH1PBE) [13] in conjunction with 6-311++G(d,p) basis set [14].

It is well known that B3 is Becke's three-parameter exchange correlation functional which uses three parameters to mix in the exact Hartree-Fock exchange correlation and LYP is the gradient-corrected correlational functional of Lee Yang and Parr that recovers dynamic electron correlation. B3LYP method is called first-generation method. On the other hand, HSEH1PBE (it is deciphered as the Heyd−Scuseria −Ernzerhof hybrid combined with Perdew, Burke, and Ernzerhof's exchange and correlation functions), which is also known as the HSE06 approach, is a second-generation method. HSE06 is a range separated hybrid functional and the slowly decaying long-ranged part of the Fock exchange interaction is replaced by the corresponding part of the PBE density functional counterpart. In the past decade, a number of studies investigating the performance of hybrid density functional theory functionals reported that HSEH1PBE level gives very accurate results for both organic molecules and organometallic complexes [15–18]. So, we decided to use both B3LYP and HSEH1PBE levels in order to make a comparison and provide more reliable results for geometric parameters, spectroscopic, electronic, and nonlinear optical properties of investigated structure. These calculations were performed by GAUSSIAN 09 program [19], and the visualization parts were conducted using GaussView 5 [20] program. The optimized structures and vibration spectra of NMPMN [6] were determined by using B3LYP and HSEH1PBE theory levels. The frequency values were computed by DFT levels that contain well-known systematic errors. Thus, the scaling factor of 0.9899 was used for both theory levels in order to repair discrepancies between experimental and theoretical results [21]. The detailed assignments of vibrational frequencies were made by the aid of potential energy distribution (PED) analysis with VEDA [22, 23]. DFT levels were also used to calculate the dipole moment (μ), mean polarizability ($<\alpha>$), anisotropy of the polarizability ($\Delta\alpha$), and first static hyperpolarizability ($<\beta>$) [24]. Additionally, highest occupied molecular orbital (HOMO)-lowest unoccupied molecular orbital (LUMO) energies and molecular charges of title molecule were also investigated.

2 Results and Discussion

2.1 Geometric Structural Parameters of NMPMN Molecule

The optimized molecular structure of NMPMN was calculated by using DFT/B3LYP and DFT/HSEH1PBE theory levels with 6-311++G (d,p) basis set. The illustrations of NMPMN are given in Fig. 1. The title compound was synthesized by Naseema et al. [6], but the crystal structure parameters such as bond lengths and bond angles were not presented. In the paper, therefore, experimental parameters of the analogous molecules [25, 26] were selected to compare with theoretical results which are given in Table 1. The experimental bond lengths of C-N, C=O, and N=O were reported 1.441, 1.250, and 1.232 Å [25, 26]. The calculated values of corresponding bond lengths 1.481, 1.222, and 1.224 Å at B3LYP and 1.471, 1.218, and 1.214 Å at HSEH1PBE theory level were obtained. The bond angles O-N-O and C-N-O were observed at 122.6° and 122.5° [25, 26]. These angles were computed circa 125.0° and 117.5° with both theory levels. When compared to experimental results [6], theoretical methods estimate systematically longer bond lengths. However, it should be noted that the experimental results belong to solid phase and the theoretical calculations belong to gas phase.

2.2 Vibrational Assignments of NMPMN

The vibrational data of NMPMN molecule are tabulated in Table 2. The free N-H stretching vibration is observed in the region of 3600–3400 cm^{-1}. The experimental N-H stretching band appeared at 3353 cm^{-1} [6]. The computed wavenumber for this vibration was found 3500 cm^{-1}(B3LYP) and 3529 cm^{-1} (HSEH1PBE). The asymmetric and symmetric C-H stretching vibrations of methyl group are assigned at 3033 cm^{-1} [6]. These bands were calculated in the region of 2984–2906 cm^{-1}. The IR active bands at 1531 and 1293 cm^{-1} were assigned to asymmetric and symmetric N-O stretching vibrations of NMPMN molecule, which were calculated at 1519 and 1317 cm^{-1} (B3LYP) and 1564 and 1371 cm^{-1} (HSEH1PBE). The amide carbonyl group and aromatic C=C stretching vibrations are observed at 1653 and 1560 cm^{-1} [6].

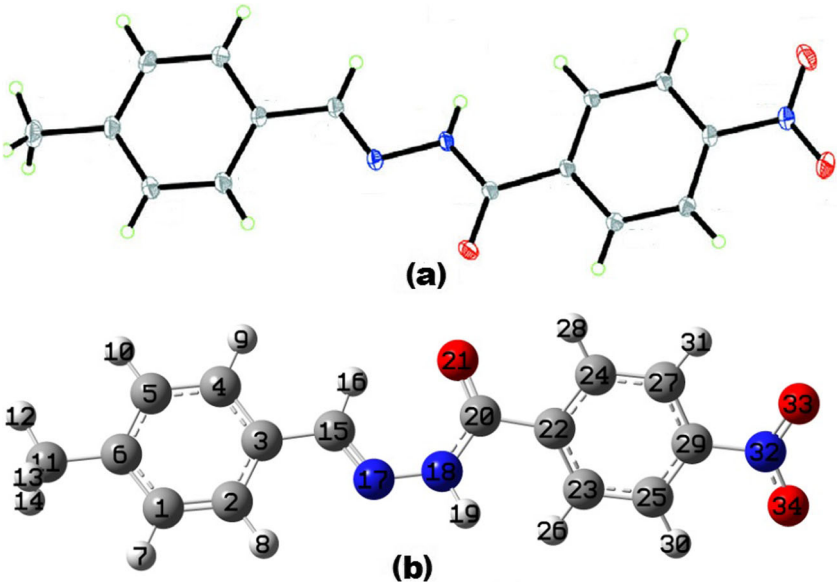

Fig. 1 **a** Experimental structure and **b** theoretical structure of the title compound

The corresponding bands were calculated at 1658 and 1571 cm^{-1} in B3LYP and 1606 and 1566 cm^{-1} in HSEH1PBE theory levels. The identification of C=N and C-N vibrations is rather difficult since the mixing of vibrations possible in this region. However, with help of theoretical calculations, the band at 1613 cm^{-1} was assigned to C=N stretching vibration.

Table 1 The bond lengths (Å) and angles (°) of the title compound B3LYP/6-311++G(d,p) and HSEH1PBE/6-311++G(d,p)

Parameters	Experimental [25, 26]	Theoretical	
		B3LYP	HSEH1PBE
Bond lengths (Å)			
C29-N32	1.441	1.481	1.471
C20-O21	1.250	1.222	1.218
N32-033	1.232	1.224	1.214
N32-034	1.232	1.224	1.214
C20-N18	1.357	1.374	1.367
C15-N17	1.341	1.287	1.283
N17-N18	1.379	1.373	1.359
N18-H19	0.960	1.000	1.000
Bond angles (°)			
O34-N32-O33	122.6	124.9	125.1
C29-N32-O33	122.5	117.5	117.4
N32-C29-C28	114.4	118.9	118.8
C25-C29-C27	121.7	122.1	122.3
C23-C22-C24	117.3	119.5	119.7
C20-N18-H19	114.1	117.9	117.7
N17-N18-C20	126.2	130.9	130.6
N18-N17-C15	126.2	121	121.1

2.3 NMR studies of NMPMN

The computer simulation methods offer a powerful way to predict and interpret the structure of large molecules. Gauge-independent atomic orbital (GIAO) which is one of the most common approach was performed to calculate the nuclear

Table 2 The experimental and calculated vibration frequencies of the title compound

Assignments	Wavenumbers (cm^{-1})		
	Experimental [6]	Theoretical	
		B3LYP	HSEH1PBE
υ(C-H)sym	3033	3099	3090
		3072	3072
		3051	3055
		2906	2927
υ(C-H)asym	3033	3098	3117
		3080	3098
		3056	3074
		3043	3058
		3035	3057
		2984	3016
		2952	2986
υ(N-H)	3353	3500	3529
υ (N-O2)asym	1531	1519	1564
υ (N-O2)sym	1293	1317	1371
υ(C=C)amid	1653	1658	1606
υ(C=N)	1613	1597	1598
υ(C=C)aro	1560	1570	1566

υ stretching, *asym* asymmetric, *sym* symmetric, *aro* aromatic ring, *amid* amide carbonyl group

magnetic shielding tensors. The isotropic shielding values were used to calculate the isotropic chemical shifts with respect to tetramethylsilane (TMS).The theoretical ^{1}H and ^{13}C NMR chemical shifts of NMPMN were performed by the means of B3LYP and HSEH1PBE theory levels with 6-311++G(d,p) basis set. The ^{1}H and ^{13}C NMR chemical shifts are summarized in Table 3.

It is well known that aromatic carbons give signals at in the range of 100–150 ppm [23]. ^{13}C chemical shifts for all calculations were in the range of 168.47−26.84 ppm at B3LYP level and 169.65 to−25.68 ppm at HSHE1PBE level with 6-311++G (d,p) level of the title molecule. In our calculations, the calculated C20, C15, and C29 were higher than 150 ppm due to the electronegativity features of N and O atoms.

^{1}H chemical shift for all calculations were at the range of 11.49–2.67 ppm (B3LYP) and 11.39–2.74 ppm (HSEH1PBE). The NMR peak of hydrogen attached or nearby electron withdrawing atom or group appears in the downfield. The proton signal originating from H16 was calculated at 11.49 ppm for B3LYP and 11.39 ppm for HSEH1PBE. Since the H31 and H30 protons nearer to electron withdrawing NO_2 group than H28 and H26 protons, these protons give peaks at the more downfield region. The other aromatic protons H7, H8, H9, and H10 give signals in expected regions [27]. In this research, we have reported NMR spectral data of title molecule to understanding chemical and nonlinear optical properties of NMPMN.

2.4 Electronic properties of NMPMN

The electronic absorption basically means the transition from the ground to the first excited state and is mainly described by one electron transitions from the HOMO to the LUMO. In other words, HOMO is the orbital that acts as an electron donor, whereas LUMO is an orbital that acts as electron acceptor. The energy values of HOMO and LUMO and their energy gap reflect the chemical activity of the molecules. The energy gap between HOMO and LUMO has been used to prove the bioactivity from intramolecular charge transfer [28].

HOMO and LUMO energies were calculated as − 6.4641 and − 3.2486 eV for HSEH1PBE level while − 6.4422 and − 3.1480 eV for B3LYP level, respectively. It can be seen from Fig. 2 that the energy band gap between the HOMO and LUMO orbitals was predicted as 3.2155 eV by using B3LYP/6-311++G (d, p) method. The mentioned value was calculated as 3.2942 eV by using HSEH1PBE/6-311++G (d,

Table 3 Experimental and theoretical chemical shift of the title compound

Atom	Exp.[6]	Theoretical		Atom	Exp. [6]	Theoretical	
		B3LYP	HSEH1PBE			B3LYP	HSEH1PBE
^{1}H				^{13}C			
43-H	14.4	15.17	13.66	3-C	205.23	194.41	191.58
41-H		14.76	13.17	31-C		193.75	190.90
6-H	5.60	6.32	5.87	25-C	181.17	186.65	184.60
35-H		6.24	5.75	11-C		185.47	183.12
23-H		4.87	4.46	5-C		176.43	173.71
18-H		4.16	3.79	34-C		175.31	172.63
17-H	3.60	3.97	3.62	1-C	169.18	170.07	167.55
24-H		3.66	3.33	32-C		169.64	167.15
29-H	3.40	3.48	3.14	4-C	121.18	115.04	113.38
28-H		3.47	3.13	33-C		114.87	113.12
14-H		3.36	3.10	30-C	101.46	107.53	104.62
15-H		3.35	3.05	2-C	99.000	106.03	103.04
27-H		3.32	3.04	16-C	30.8	48.53	45.76
9-H	2.87	2.86	2.53	22-C		47.09	44.31
20-H		2.86	2.51	19-C		36.98	34.47
8-H		2.82	2.50	36-C	29.97	24.97	24.13
38-H		2.82	2.50	7-C		24.93	24.07
39-H		2.75	2.47	12-C	20.69	23.70	22.89
13-H		2.69	2.37	26-C		23.13	22.36
21-H	2.00	2.46	2.20				
10-H		2.42	2.18				
37-H		2.33	2.07				

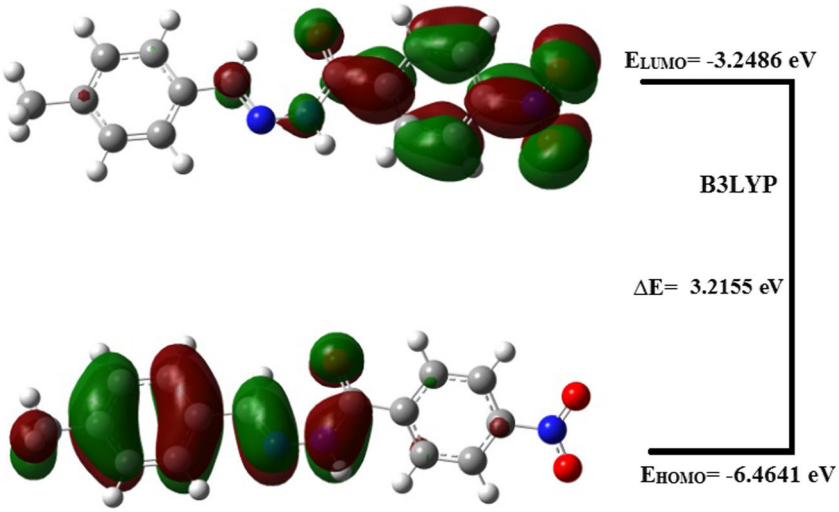

Fig. 2 HOMO and LUMO energies of the title compound

p) method. Low levels of HOMO–LUMO energy gap can give rise to the more charge transportation.

2.5 Electrical properties of NMPMN

The intramolecular charge transfer from the electron donating group to the electron withdrawing group through single-double bond can induce large variations of both the molecular dipole moment as and the molecular polarizability, making IR and Raman activities strong at the same time. The C=O, C-N, and C=C stretching vibrations were found to be strong and simultaneously active in IR. Additionally, the movement of π electron from donating group to the withdrawing group makes the highly polarizable molecule. Accordingly, intramolecular charge transfer interactions might be responsible for the nonlinear optical (NLO) properties. NLO properties get enhanced by the substitution of molecule with carbonyl and hydroxyl groups which are involved in hydrogen bond interactions.

We investigate the values of the total static dipole moment (μ), the mean polarizability ($<\alpha>$), the anisotropy of the polarizability ($\Delta\alpha$), and the mean first-order hyperpolarizability ($<\beta>$) which were calculated as follows [24],

$$\mu = \left(\mu_x^2 + \mu_y^2 + \mu_z^2\right)^{1/2} \quad (1)$$

$$\langle\alpha\rangle = \left(\alpha_{xx} + \alpha_{yy} + \alpha_{zz}\right)/3 \quad (2)$$

$$\Delta\alpha = \left(\left[\left(\alpha_{xx}-\alpha_{yy}\right)^2 + \left(\alpha_{yy}-\alpha_{zz}\right)^2 + \left(\alpha_{zz}-\alpha_{xx}\right)^2\right]/2\right)^{1/2} \quad (3)$$

$$\beta = \left(\beta_x^2 + \beta_y^2 + \beta_z^2\right)^{1/2} \quad (4)$$

Table 4 presents obtained NLO parameters for the title compound compared with those for *para*-nitro-aniline (pNA) molecule [29, 30] which is a typical NLO material. These values were calculated by using B3LYP at 5.1724 Debye, 36.6×10^{-24} esu, and 41.1×10^{-24} esu, respectively. In addition, mentioned values are 4.9422 Debye, 36.1×10^{-24} esu, and 40.5×10^{-24} esu, with HSEH1PBE, respectively. As seen in these values, high β can be explained by a slight rise in the donor strength of the title molecule, which also red shifts the charge-transfer transition and thus rising the near-resonance enhancement of β [31–33].

2.6 Molecular surfaces of NMPMN

Molecular electrostatic potential (MEP) was used in order to grasp the molecular interactions. MEP has been established extensively as a useful quantity to explain the hydrogen bonding, reactivity, and structure activity of molecular systems [34]. The three-dimensional distribution of MEP was very helpful in that negative regions can be regarded as nucleophilic centers, whereas regions with positive electrostatic potential were potential electrophilic sites. Moreover, the electrostatic potential made the polarization of the electron density visible [33]. The MEP surface which was a plot of electrostatic potential mapped onto the iso-electron density surface simultaneously displays molecular shape, size, and electrostatic potential values [34]. The color scheme for the MEP surface was red electron-rich or partially negative charge, blue electron-deficient or partially positive charge, light blue-slightly electron-deficient region, and yellow slightly electron-rich region, respectively. Areas of low potential, represented by red, were characterized by an abundance of electrons. Areas of high potential, represented by blue, were characterized by a relative absence of electrons. To predict reactive sites for electrophilic and nucleophilic attack for the title molecule, the 3D plot of MEP simulated by using B3LYP and HSEH1PBE levels with 6-311++ G(d) basis set is given in Fig. 3. The polarization effect is clearly visible in Fig. 3.

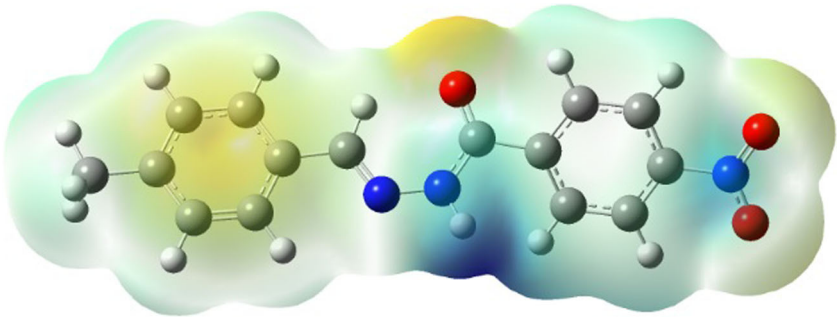

Fig. 3 The molecular electrostatic potential (MEP) surface of the title compound

2.7 Mulliken Charge and NBO analysis of NMPMN

Atomic charges and charge transfer were used as a concept in chemical reasoning about molecular behavior and reactivity. Thus, atomic charges continue to play an important role in quantum chemistry and much research continues to being done to refine the concept of an atomic charge. Since the description of charge populations of atomic orbitals by Mulliken [35] were widely used tools for the interpretation of the internal structure of molecular orbitals, it is clear that Mulliken populations yield one of the simplest pictures of charge distribution and Mulliken charges render net atomic populations in the molecule [34]. The Mulliken charge distributions of the title molecule has been calculated at B3LYP/6-311++G (d,p) and HSEH1PBE/6-311++G(d,p) methods. The results are given in Fig. 4. As can be seen from the Fig. 4, the magnitudes of the carbon Mulliken charges, found to be either positive or negative, were noted to change from − 0.698258 to 0.803743 for title molecule. Since the C3 and C23 carbon atoms have higher positive charge than other carbons. The H19 atom exhibited the largest positive charge among hydrogen atoms due to the bounding to N atom.

The natural bond analysis is performed to understand various second-order interactions between the filled orbitals of one subsystem and vacant orbitals of another subsystem, which is a measure of the intermolecular delocalization or hyperconjugations. NBO analysis gives information about the intermolecular and intramolecular bonding, besides interactions among bonds [35].

To identify the NBO second-order perturbation stabilization energy $E^{(2)}$, the following parameters are used:

$$E^{(2)} = \Delta E_i j = q_i \frac{F(i.j)^2}{\varepsilon_j - \varepsilon_i'} \quad (5)$$

where q_i is the donor orbital occupancy, ε_i and ε_j are diagonal elements, and F (i,j) is the off-diagonal NBO matrix element.

Table 5 provides an overview of the possible intense interactions. Table 5 indicates that there is a strong hyperconjugative interaction π^* (C22-C23) → π^* (C24-C27) and π^* (N32-O33) → σ^* (N32-O33) for the title molecule, and their interaction energies were found as 160.05 and 163.59 kcal mol^{-1} for HSEH1PBE method, respectively. The energy contributions of LP1 (N18) → π^* (C20-O21) and LP2 (O21) → σ^* (N18-C20) interactions were calculated as 63.80 and 27.13 kcal mol^{-1} for HSEH1PBE method. In addition, it is important to recognize that there is a possibility for delocalization of alone pair (LP) of electrons. It is likely that the strong delocalization is a result of the electron density of conjugated bond of aromatic ring.

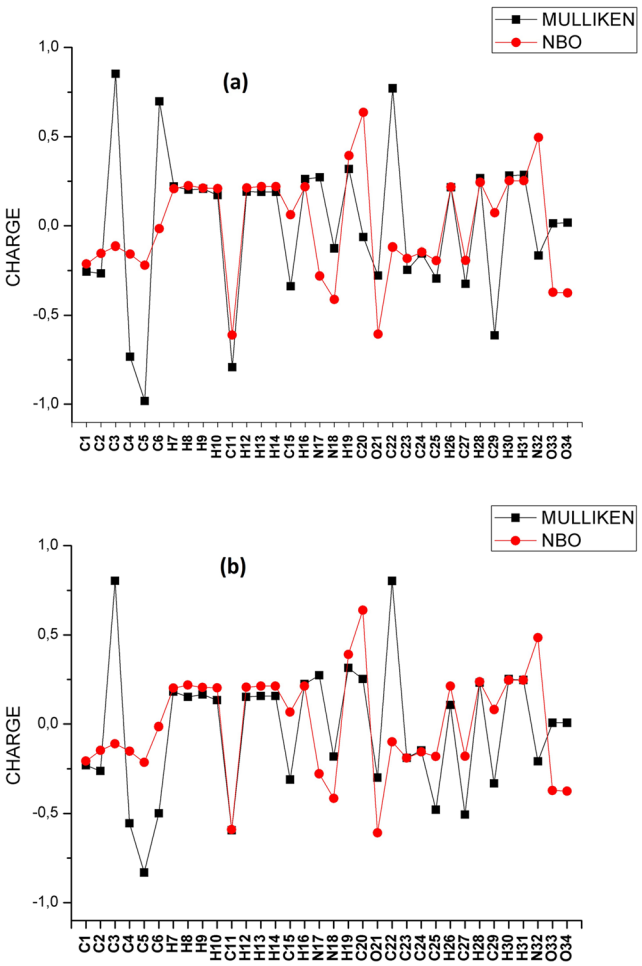

Fig. 4 Comparative of Mulliken and NBO plots of the title compound. **a** B3LYP/6-311++G(d,p). **b** HSEH1PBE/6-

Table 4 Nonlinear optical property values of the title compound

Property	B3LYP	HSEH1PBE
μ	5.1724	4.9422
μ	2.44a	2.44a
$<\alpha>$	36.6	36.1
$\Delta\alpha$	41.1	40.5
$<\alpha>$	22b	22b
$<\beta>$	69.1	60.6
$<\beta>$	15.5c	15.5c

Total static dipole moment (μ, in Debye), the mean polarizability ($<\alpha>$, in 10–24 esu), the anisotropy of the polarizability ($\Delta\alpha$, in 10–24 esu), and the mean first-order hyperpolarizability ($<\beta>$, in 10–30 esu) for the all of columns. a, b, and c are theoretically defined values for *para*-nitro-aniline (pNA) molecule

Table 5 Second-order perturbation theory analysis of the Fock matrix in NBO basis of the title compound

Type	Donor	Type	Acceptor	$E^{(2)}$ (kcal mol^{-1})	
				B3LYP	HSEH1PBE
π	C1-C2	π*	C3-C4	18.23	17.11
π	C1-C2	π*	C5-C6	21.04	19.84
π	C3-C4	π*	C1-C2	19.24	18.27
π	C3-C4	π*	C5-C6	18.13	17.04
π	C3-C4	π*	C15-N17	20.44	20.01
π	C5-C6	π*	C1-C2	17.41	16.34
π	C5-C6	π*	C3-C4	22.25	20.79
π	C22-C23	π*	C20-O21	14.31	19.29
π	C22-C23	π*	C24-C27	17.11	16.12
π	C22-C23	π*	C25-C29	22.43	23.04
π	C24-C27	π*	C22-C23	21.74	20.26
π	C24-C27	π*	C25-C29	21.68	16.26
π	C25-C29	π*	C22-C23	18.14	18.03
π	C25-C29	π*	C24-C27	18.73	38.73
π	N32-O33	LP(3)	O34	11.65	12.03
LP(1)	N18	π*	C15-N17	25.28	26.17
LP(1)	N18	π*	C20-O21	54.89	63.80
LP(2)	O21	σ*	N18-C20	25.32	27.13
LP(2)	O21	σ*	C20-C22	18.79	18.36
π*	C15-N17	π*	C3-C4	69.15	68.79
π*	C22-C23	π*	C24-C27	158.67	160.05
π*	C25-C29	π*	C24-C27	120.96	113.01
σ*	C29-N32	π*	N32-O33	68.27	66.37
π*	N32-O33	σ*	C27-H31	57.41	63.32
π*	N32-O33	σ*	N32-O33	156.26	163.59
π*	N32-O33	σ*	N32-O34	102.31	109.53

$E^{(2)}$ means energy of hyperconjugative interactions (stabilization energy)

3 Conclusions

In this study, molecular structure, natural bonding orbital (NBO) analysis harmonic vibrational frequencies, ^{1}H and ^{13}C NMR chemical shifts, HOMO and LUMO energy analysis, molecular electrostatic potential maps (MEP), Mulliken charges and the natural bonding orbital (NBO), electric dipole moment (μ), polarizability (α), the first-order hyper polarizability (β), and electronic and thermodynamic properties of the title molecule have been calculated by using HSEH1PBE/6-311++G(d,p) and B3LYP/6-311++G(d,p) methods. The small differences were observed between the theoretical and experimental structural parameters and the vibrational wavenumbers. However, it should be noted that the experimental section was performed in solid phase while theoretical calculations were performed in gas phase. NBO analysis was carried out by B3LYP method in detail. NBO analysis indicated that there are strong hyperconjugative interactions that resulted in intramolecular charge transfer causing stabilization of the title molecule. Nonlinear optical behavior of the examined compound was investigated by the determination of the electric dipole moment μ, the polarizability α, and the hyperpolarizability β using B3LYP methods. So, it is demonstrated that the investigated compound can be used as a NLO material.

References

1. P.N. Prasad, D.J. Williams, *Introduction to Nonlinear Optical Effects in Organic Molecules and Polymers* (Wiley, New York, 1991)
2. D.S. Chemla, J. Zyss, *Nonlinear Optical Properties of Organic Molecules and Crystals* (Academic Press, New York, 1987)
3. Y. Iitaka, Acta Crystallogr. **14**, 1 (1961)
4. R. Christian, *Solvents and Solvent Effects in Organic Chemistry* (VCH, New York, 1990)
5. H. Ringertz, Acta Crystallogr. B **27**, 285 (1971)
6. K. Naseema, V. Rao, K.V. Sujith, B. Kalluraya, Current Applied Phys. **10**, 1236 (2010)
7. A.E. Reed, L.A. Curtiss, F. Weinhold, Chem. Rev. **88**, 899 (1988)
8. N. Öner, Ö. Tamer, D. Avcı, Y. Atalay, Acta A **133**, 542 (2014)
9. H. Pir, N. Günay, Ö. Tamer, D. Avcı, Y. Atalay, Acta A **112**, 331 (2013)
10. Ö. Tamer, D. Avcı, Y. Atalay, Acta A **136**, 644 (2015)
11. A.D. Becke, J. Chem. Phys. **98**, 5648 (1993)
12. C. Lee, W. Yang, R.G. Parr, Phys. Rev. B **37**, 785 (1988)
13. J. Heyd, G. Scuseria, J. Chem. Phys. **121**, 1187–1192 (2004)
14. M.J. Frisch, J.A. Pople, J.S. Binkley, J. Chem. Phys. **80**, 3265–3269 (1984)
15. S. Altürk, D. Avcı, Ö. Tamer, Y.Atalay, J. Organomet. Chem. **797**, 110–119 (2015).
16. D. Avcı, Ö. Tamer, S. Bahçeli, Y. Atalay, Can. J. Chem. **93**, 1147–1156 (2015).
17. S. Altürk, D. Avcı, Ö. Tamer, Y.Atalay, Comput. Theor. Chem. **1100**, 34–45 (2017).

18. K. Avhad, A. Jadhav, N. Sekar, J. Chem. Sci. **129**(12), 1829–1841 (2017)
19. M.J. Frisch, G.W. Trucks, H.B. Schlegel, G.E. Scuseria et al., *Gaussian, Inc., Wallingford CT Gaussian 09, Revision A.1* (Gaussian, Inc., Wallingford CT, 2009)
20. R. Dennington, T. Keith, J. Millam, Semichem Inc., Shawnee Mission KS, GaussView, Version 5, (2009)
21. D. Avcı, Y. Atalay, Int. J. Quantum Chem. **109**, 328 (2009)
22. M.H. Jamroz, J.C. Dobrowolski, J. Mol. Struct. **475**, 565–566 (2001)
23. M.H. Jamroz, Vibrational Energy Distribution Analysis VEDA4, Warsaw, (2004)
24. D. Avcı, A. Başoğlu, Y. Atalay, Int. J. Quantum Chem. **111**, 130 (2011)
25. Ö. Tamer, D. Avcı, Ç. Arıoğlu, A. Başoğlu, Y. Atalay, Indian J. Phys. (2014)
26. T. Dhanabal, G. Amirthaganesan, M. Dhandapani, S.K. Das, J. Mol. Struct. **1035**, 483 (2013)
27. M.A. Fersi, I. Chaabane, M. Gargouri, A. Bulou, Indian J. Phys. **90**, 381 (2016)
28. E. Tarcan, A. Pekparlak, D. Avcı, Y. Atalay, Arab. J. Sci. Eng. **34**, 55 (2009)
29. L.T. Cheng, W. Tam, S.H. Stevenson, G.R. Meredith, G. Rikken, S.R. Marder, J. Phys. Chem. **10631**, 95 (1991)
30. P. Kaatz, E.A. Donley, D.P. Shelton, J. Chem. Phys. **108**, 849–856 (1998)
31. W. Wenseleers, E. Goovaerts, P. Hepp, M. Helena Garcia, M. Paula Robalo, A.R. Dias, M.F.M. Piedade, M. Teresa Duarte, Chem. Phys. Lett. **367**, 390 (2003)
32. V. Mukherjee, N. Singh, R.A. Yadav, Spectrochim. Acta A **73**, 249 (2009)
33. I. Fleming, *Frontier Orbitals and Organic Chemical Reactions* (John Wiley and Sons, New York, 1976)
34. R.S. Mulliken, J. Chem. Phys. **23**, 1833 (1955)
35. F. Weinhold, C.R. Landis, *Valency and Bonding: a Natural Bond Orbital Donor–Acceptor Perspective* (Cambridge University Press, Cambridge, 2005)